INVESTIGATING POSSIBLE CAUSES OF LIGHT INDUCED DEGRADATION IN BORON-DOPED FLOAT-ZONE SILICON

D. Sperber, A. Herguth, G. Hahn
University of Konstanz, Department of Physics, 78457 Konstanz, Germany

ABSTRACT: The use of different silicon nitride deposition tools is found to change the degree of light induced degradation (LID) of B-doped float-zone silicon after a fast firing step. In addition, a thermally grown SiO_2 interlayer further suppresses LID after firing. Possible mechanisms and a potential link to Light and elevated Temperature Induced Degradation (LeTID) are discussed. Furthermore, it is shown that LID is not related to an earlier described class of thermally activated defects in float-zone silicon and that phosphorous gettering does not influence the occurrence of LID in B-doped float-zone silicon significantly.
Keywords: Light induced degradation, LeTID, Stability, Degradation, Silicon nitride, Minority carrier lifetime

1 MOTIVATION

Light and Elevated Temperature Induced Degradation (LeTID) is a subtype of light induced degradation (LID) and poses a significant challenge as it may severely limit bulk minority charge carrier lifetime τ_b in multicrystalline silicon (mc-Si) [1-3]. Highly purified B-doped float-zone silicon (FZ-Si), on the other hand, has been shown to suffer from LID, too, after a fast firing step [4-6]. There are a number of similarities between LID in mc-Si and FZ-Si, leading to the question whether LID in FZ-Si is connected to LeTID.

Only recently, it has been supposed that LeTID also affects monocrystalline Czochralski-grown silicon (Cz-Si) [7,8], giving rise to the idea that LeTID affects crystalline silicon in general. If LeTID also affects B-doped FZ-Si, this would offer the possibility to study LeTID in a well controlled and highly purified material. Hence, the aim of this contribution is to further investigate possible root causes of LID in FZ-Si and compare it to LeTID.

2 EXPERIMENTAL

All shown samples are made of B-doped FZ-Si wafers of thickness 250 µm and specific resistivity ~1 Ωcm, equaling a doping density N_d of ~$1.5 \cdot 10^{16}$ cm^{-3}. The wafers already received a saw damage etch and chemical clean by the manufacturer and were shipped with a thin chemically grown oxide on the wafer surface. Part of the wafers did not receive further chemical pre-treatment while others were subjected to a dip in hydrofluoric acid (HF) to remove the thin oxide. Selected samples received a clean in a solution of H_2O_2 and H_2SO_4 at 80°C, followed by another dip in HF (Piranha clean).

Two different plasma enhanced chemical vapor deposition (PECVD) tools were used for two-sided deposition of SiN_x:H. A type 1 SiN_x:H was grown in a lab-tool using a direct plasma at a frequency of 13.56 MHz. The deposition temperature was 400°C and a two-sided deposition took ~20 min. Type 2 SiN_x:H was grown in an industrial direct plasma tool with a frequency of 40 kHz. In this case, the deposition temperature was 450°C and a two-sided deposition took ~1.5 h. Accordingly, samples with different SiN_x:H deposition have seen a different temperature load during processing. Both SiN_x:H depositions resulted in a refractive index ~2.0 (600 nm) and thickness ~75 nm. As precursor gases, NH_3 and SiH_4 were used in both PECVD tools, resulting in a hydrogen-rich SiN_x:H layer in both depositions.

Afterwards, most samples were laser-cut into square samples of edge length 5 cm. Most samples were then fired at a measured peak sample temperature ~800°C in a fast firing belt furnace. Two samples were, however, fired as part of a whole wafer and the temperature measurement might have underestimated the real wafer temperature. In this case, firing temperatures are indicated as ≥800°C. After firing, samples were stored in darkness until LID treatments started.

LID treatments were carried out on illuminated hotplates at 80°C and ~1 sun equivalent illumination intensity, achieved by matching the short circuit current of a solar cell to that under a solar spectrum simulator [9]. During treatment, effective minority carrier lifetime τ_{eff} was repeatedly determined by photoconductance decay, using a Sinton Instruments lifetime tester (WCT-120). One sample was additionally characterized with photoluminescence (PL) imaging at different points of sample treatment.

3 RESULTS

3.1 Influence of different SiN_x:H on LID in FZ-Si

Two samples which received no further chemical pre-treatment were coated with different types of SiN_x:H before firing at ~800°C. The results of subsequent LID treatment at 80°C and ~1 sun are shown in Fig. 1. As can be seen, τ_{eff} reaches a minimum, denoted with the roman number I, after ~1 h of treatment in both samples. Feature I has previously been shown to be caused by degradation of τ_b, and a subsequent regeneration of τ_b then leads to a maximum II of τ_{eff} [4]. The subsequent long-term decline of τ_{eff} has been shown to be caused by a decrease of surface passivation quality [4,10] and will not be the focus of this paper.

As can be seen, feature I is significantly stronger in the sample which received a type 2 SiN_x:H. This is also visible in the change of effective defect density ΔN_{eff} (Fig. 2) which was calculated with reference to the first measurement point after treatment started to exclude initial effects of illuminating a sample (*e.g.* changing the state of FeB complexes):

$$\Delta N_{eff}(t) = 1/\tau_{eff}(t) - 1/\tau_{eff}(t_1)$$

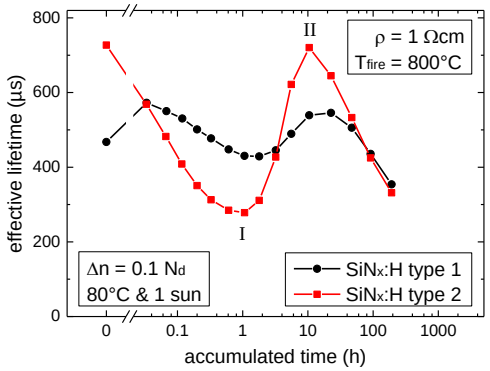

Figure 1: Evolution of τ_{eff} at injection level $\Delta n = 0.1\ N_d$ of two samples that differed in SiN_x:H deposition only and were treated simultaneously at 80°C and ~1 sun.

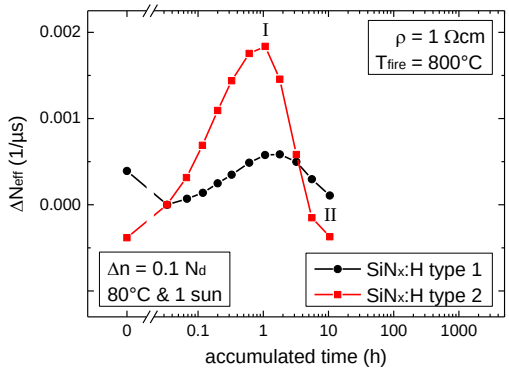

Figure 2: Evolution of ΔN_{eff} ($\Delta n = 0.1\ N_d$) of the samples shown in Figure 1.

So far, measurement data were only evaluated at $\Delta n = 0.1\ N_d$. In [11], an injection dependent visualization has been introduced to show a wide injection range of measurement data while still providing good temporal resolution as well. The injection resolved plots of the samples discussed before are shown in Figs. 3 and 4 and provide additional information: It can be seen that the biggest difference of degradation at feature I can be found at lower injection (blue) in accordance with stronger Shockley-Read-Hall recombination in the FZ bulk. The values at higher injection (red) and a calculation of the surface saturation current density J_{0s} additionally reveal that the sample with type 1 deposition suffers from more surface related recombination, explaining the lower τ_{eff} before sample treatment and at feature II.

Because both samples did not receive a chemical pre-treatment and differ in the PECVD step only, this step should have caused the different degradation behavior. One possible difference lies in a different hydrogenation of the samples. Hydrogen has been speculated to be involved in LID of FZ-Si [4,6], and it is known that different PECVD deposition temperatures result in a different degree of hydrogenation of the silicon bulk in a subsequent high temperature step [12]. Additionally, another substance besides hydrogen may affect LID via in- or out-diffusion during the firing step.

Aside from diffusion related differences, the samples have also seen a different temperature load during processing due to different deposition temperature and duration. It is therefore possible as well that a different degradation behavior arises due to different temperature load and future experiments should aim on varying

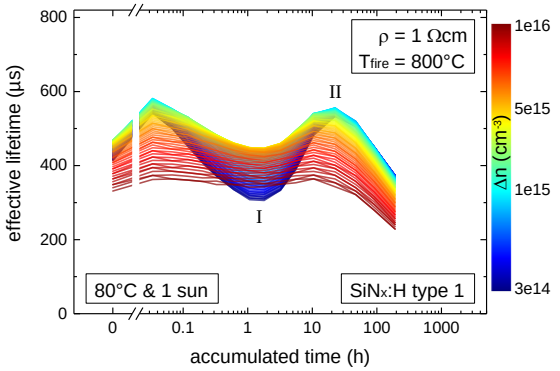

Figure 3: Injection resolved evolution of τ_{eff} of the sample with type 1 SiN_x:H. Δn is color coded, ranging from lower injection (blue) to higher injection (red).

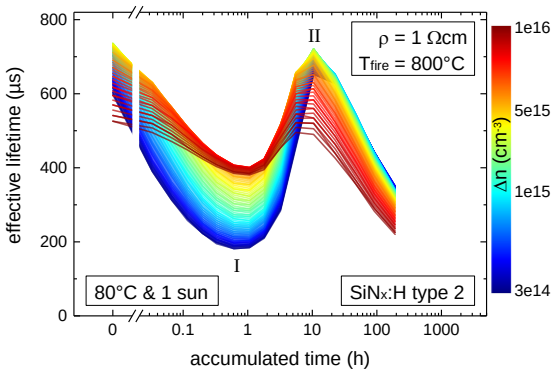

Figure 4: Injection resolved evolution of τ_{eff} of the sample with type 2 SiN_x:H.

temperature load independent of SiN_x:H deposition type to further investigate a possible influence of temperature load on LID behavior.

3.2 Influence of 1000°C anneal and $POCl_3$ gettering

In [13] it has been shown that both B-doped and P-doped FZ-Si may suffer from thermally activated defects after being treated in a temperature range between ~400°C and ~800°C. However, this type of defects can be permanently annihilated by annealing a sample at a temperature ≥1000°C [13]. To investigate a possible link between these thermally activated defects and LID in FZ-Si, the sample shown in Fig. 5 first received a 1000°C anneal in oxygen ambient for 30 min before receiving an HF dip and a Piranha clean. After a type 2 deposition and firing, the sample still shows significant LID.

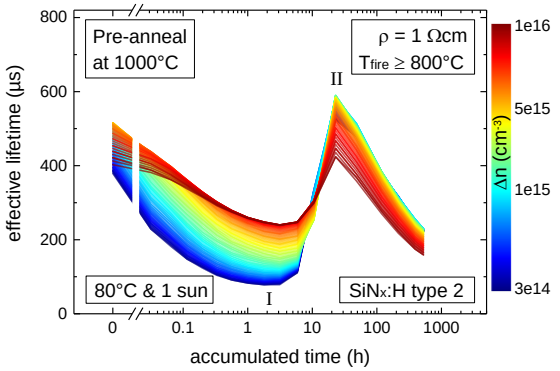

Figure 5: Injection resolved evolution of τ_{eff} of a sample passivated with type 2 SiN_x:H. The sample received an anneal at 1000°C for 30 min before sample processing.

Degradation is even stronger as in the samples discussed before which is probably related to a slightly higher firing temperature of the sample. Consequently, it can be stated that LID is not related to thermally activated defects as discussed in [13]. A similar conclusion has been drawn in [6] concerning AlO_x:H/SiN_x:H passivated samples.

Another sample first received a $POCl_3$ diffusion (840°C for ~45 min) which may getter impurities. After etching off the resulting emitter, the sample received a Piranha clean and a type 2 SiN_x:H before firing. The sample shows a very similar degradation behavior compared to samples without gettering step (data not shown), leading to the conclusion that the defects responsible for LID in FZ-Si are not significantly influenced by a $POCl_3$ gettering step.

3.3 Influence of SiO_2 interlayer

Another sample was passivated with a layer stack consisting of 10 nm SiO_2 (thermally grown at 840°C for 20 min) capped with type 2 SiN_x:H. As can be seen in Fig. 6, this sample shows no significant bulk related degradation (no dip in blue). The sample received a Piranha clean before thermal oxidation. However, other Piranha cleaned samples have shown strong bulk related degradation before [4,5,10]. Therefore, it appears that the thermal oxidation step caused the difference in degradation behavior. Because a phosphorous gettering step at the same temperature (840°C for ~45 min) does not significantly influence LID, as discussed in the previous section, the changed degradation behavior of the SiO_2/SiN_x:H sample is probably not related to a different temperature load. Accordingly, different hydrogenation or, more generally, diffusion-related differences are likely causes for the suppression of LID in this sample. Similar to the sample discussed here, another SiO_2/SiN_x:H sample with even better surface passivation (due to a higher oxidation temperature of 900°C) shows very weak bulk related degradation [10].

3.4 Inhomogeneous degradation behavior

One sample passivated with type 2 SiN_x:H was measured with PL imaging at different points of sample treatment. As can be seen in Fig. 7, the sample shows a rather homogeneous surface before treatment and after regeneration. Only the lower left sample corner has suffered significantly in the regenerated state (II) due to sample handling.

However, in the degraded state (I), a ring-like pattern can be observed. As the sample was cut out of the upper right part of a wafer, the ring-like pattern appears to be

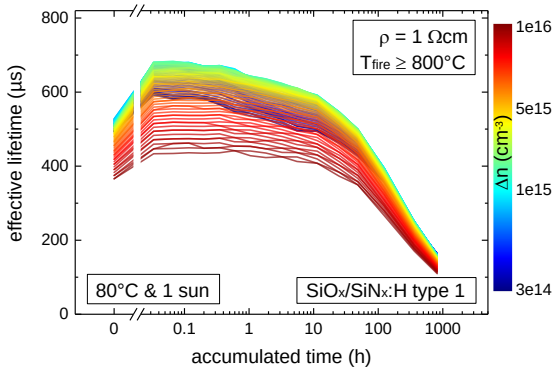

Figure 6: Injection resolved evolution of τ_{eff} of a SiO_2/SiN_x:H passivated sample (type 2 SiN_x:H).

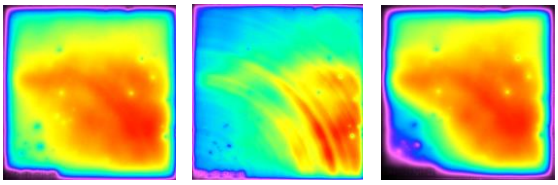

(a) before treatment (b) degraded (I) (c) regenerated (II)

Figure 7: PL images of a sample passivated with type 2 SiN_x:H, fired at ~835°C and treated at 80°C and ~1 sun (a) before treatment (b) after bulk degradation (I) and (c) after bulk regeneration (II).

concentric to the wafer center. A similar observation was made in [6] where it has been concluded that the pattern cannot occur only due to spatial inhomogeneous doping (which would cause slight variations in PL intensity) but probably reflects an inhomogeneous distribution of the defect causing LID. It remains, however, possible that slight doping variations influence the distribution of defects in the degraded state: As LID does not occur in P-doped FZ-Si [6,11], it is possible that an acceptor dopant (*e.g.* boron) takes part in defect formation. Slight variations in dopant density may then result in an inhomogeneous defect distribution.

3.5 Comparison of LID in FZ-Si with LeTID

As shown before, LID in FZ-Si may be related to the degree of hydrogenation of the silicon bulk. This possible role of hydrogen may also link LID in FZ-Si to LeTID in mc-Si: Both LID phenomena increase in strength with higher peak firing temperature [14,15] and depend on the presence of hydrogen rich layers during firing [6,16]. Accordingly, both degradation mechanisms might require an in-diffusion of hydrogen from dielectric layers into the silicon bulk during firing at elevated temperatures and possibly, LID in FZ-Si and LeTID in mc-Si share a common root cause.

If a similar mechanism is causing LID in FZ-Si and LeTID in mc-Si, further studies on FZ-Si may allow to investigate the underlying degradation mechanism in a purified and well controlled material. By optimizing dielectric deposition conditions, both temperature load and hydrogenation could be influenced to lessen the impact of LID on crystalline silicon.

4 SUMMARY

It has been shown that B-doped FZ-Si samples coated with different SiN_x:H deposition tools express a different degree of LID after a fast firing step. A SiO_2/SiN_x:H passivated sample showed no significant LID. Potential reasons for these observations include different hydrogenation of the silicon bulk and different temperature load during sample processing. Neither annihilation of thermally activated defects as described in [13] nor a gettering step influenced LID significantly. In the degraded state, an inhomogeneous distribution of the underlying defect could be observed. Finally, a potential link of LID in FZ-Si to LeTID has been discussed.

ACKNOWLEDGEMENTS

The authors would like to thank A. Heilemann, L. Mahlstaedt, J. Rinder, S. Joos, B. Rettenmaier, F. Mutter and J. Engelhardt for technical support. Part of this work was supported by the German Federal Ministry for Economic Affairs and Energy under contract numbers 0325763B and 0324001. The content is the responsibility of the authors.

REFERENCES

[1] K. Ramspeck, S. Zimmermann, H. Nagel, A. Metz, Y. Gassenbauer, B. Birkmann, A. Seidel, Proceedings 27th European Photovoltaic Solar Energy Conference (2012) 861.
[2] F. Fertig, K. Krauß, S. Rein, Physica Status Solidi RRL 9 (2015) 41.
[3] F. Kersten, P. Engelhart, H.C. Ploigt, A. Stekolnikov, T. Lindner, F. Stenzel, J.W. Müller, Solar Energy Materials and Solar Cells 142 (2015) 83.
[4] D. Sperber, A. Heilemann, A. Herguth, G. Hahn, IEEE Journal of Photovoltaics 11 (2017) 463.
[5] D. Sperber, A. Herguth, G. Hahn, Physica Status Solidi RRL 11 (2017) 1600408.
[6] T. Niewelt, M. Selinger, N.E. Grant, W. Kwapil, J.D. Murphy, M.C. Schubert, Journal of Applied Physics 121 (2017) 185702.
[7] Fertig et al., Energy Procedia 124 (2017) 338.
[8] D. Chen, M. Kim, B.V. Stefani, B.J. Hallam, M.D. Abbott, C.E. Chan, R. Chen, D.N.R. Payne, N. Nampalli, A. Ciesla, T.H. Fung, K. Kim, S.R. Wenham, Solar Energy Materials and Solar Cells 172 (2017) 293.
[9] A. Herguth, Energy Procedia 124 (2017), 53.
[10] D. Sperber, A. Graf, D. Skorka, A. Herguth, G. Hahn, IEEE Journal of Photovoltaics, accepted, doi: 10.1109/JPHOTOV.2017.2755072.
[11] D. Sperber, A. Graf, A. Heilemann, A. Herguth, G. Hahn, Energy Procedia 124 (2017), 794.
[12] H.F.W. Dekkers, G. Beaucarne, Applied Physics Letters 89 (2006) 211914.
[13] N.E. Grant, V.P. Markevich, J. Mullins, A.R. Peaker, F. Rougieux, D. Macdonald, J.D. Murphy, Physica Status Solidi A 11 (2016) 2844.
[14] D. Sperber, A. Herguth, G. Hahn, Energy Procedia 92 (2016) 211.
[15] D. Bredemeier. D. Walter, S. Herlufsen, J. Schmidt, AIP Advances 6 (2016), 035119.
[16] F. Kersten, J. Heitmann, J.W. Müller, Energy Procedia 92 (2016) 828.